Buckling of multiwalled carbon nanotubes under axial compression and bending via a molecular mechanics model

Tienchong Chang,[1,3,*] Wanlin Guo,[2] and Xingming Guo[1]
[1]*Shanghai Institute of Applied Mathematics and Mechanics, Shanghai University, Shanghai 200072, China*
[2]*Institute of Nano Science, Nanjing University of Aeronautics and Astronautics, Nanjing 210016, China*
[3]*Department of Civil Engineering, Tongji University, Shanghai 200092, China*
(Received 24 March 2005; revised manuscript received 10 June 2005; published 1 August 2005)

Based on a molecular mechanics model, analytical solutions are obtained for the critical buckling strain of multiwalled carbon nanotubes (MWNT's) under axial compression and bending. We show that only part of the outer layers buckles first while the remaining inner part remains stable in a very thick MWNT, which is quite different from the initial buckling mode of a relatively thin MWNT in which all individual tubes buckle simultaneously. Such a difference in the initial buckling modes results in quite different size effects on the critical buckling strain of thin and thick MWNT's. For instance, inserting more inner individual tubes may increase the critical buckling strain of a thin MWNT, but cannot increase the critical buckling strain of a thick tube. The effects of tube size on the initial buckling wavelength are also examined, and it is shown that the initial buckling wavelength is weakly dependent on the thickness of the MWNT.

DOI: 10.1103/PhysRevB.72.064101 PACS number(s): 61.46.+w, 62.25.+g

I. INTRODUCTION

Carbon nanotubes (CNT's) have been proposed as promising materials for superstrong bulk composites and nanoelectromechanical systems[1–5] (NEMS's) partly due to their amazing mechanical properties such as exceptional high stiffness and tensile strength and remarkable flexibility and resilience. However, direct measurement of mechanical properties of CNT's remains a challenge, and indirect methods were frequently used. As summarized by Pantano *et al.*,[6,7] most experimental measurements impose some form of bending of the CNT's and a beam theory is often used to reduce the data to an elastic modulus. For example, the elastic modulus was calculated by the measured vibration frequency or force-displacement relation of CNT's via beam models.[8–11] Buckling (often referred to as wrinkling or rippling) is often developed on the compressive side of the bend, particularly in a multiwalled nanotube (MWNT). The MWNT may be driven into nonlinear response by rippling, which results in a remarkable reduction of the measured effective bending modulus.[6,7,9,12–15] Some other physical properties such as conductance of CNT's may also be significantly changed by the occurrence of buckling.[2,16–18] Meanwhile, experimental investigations[8,9,19] have shown evidently that the buckling deformation of CNT's is completely reversible even under large strain (more than a few percent). These facts provide potential applications of the buckling of CNT's as a critical point of reversible elements in NEMS's to realize the bistate functions. It is, therefore, of significant importance to efficiently determine the critical buckling conditions of CNT's.

Both numerical simulations and analytical models have been widely used investigate buckling behavior of CNT's since it was observed experimentally.[9,20–23] Most of numerical simulations are based on molecular dynamics (MD). Iijima *et al.*[21] simulated buckling of single-walled carbon nanotubes (SWNT's) and MWNT's under bending and gave a quantitative explanation of their experimental observations. Yakobson *et al.*[24] studied buckling of SWNT's under axial compression, bending, and torsion and showed that the buckling behavior of a SWNT can be well predicted by a continuum shell model which provides very concise expressions for the critical buckling conditions of SWNT's. Srivastava and Barnard[25] calculated axial buckling of a (10, 10) SWNT and a $(5n,5n)_{n=4-7}$ MWNT's by large-scale MD simulations. Garg *et al.*[26] studied the buckling behavior of the nanotube as a probe tip of the atomic force microscope (AFM), and the effects of tube length and surface type on the mechanisms of the interaction of tubes with surfaces were investigated. Recently, the effects of tube size, chirality, temperature, and intertube van der Waals (vdW) interactions on the buckling of CNT's were studied.[16,27–30] MD simulations may, in principle, be used to investigate any atomic system if the interactions between atoms could be determined. Nevertheless, direct simulation of systems with a large number of atoms, such as large thick MWNT's, seems prohibitive for the demanded computational cost. To our knowledge, no direct MD simulation for the mechanical behavior of MWNT's with layers more than 5 is reported in the literature. As an alternative, two- and three-dimensional finite-element analyses of bent MWNT's were conducted[12,31] to investigate the effect of rippling on the effective bending modulus of the thick MWNT's. The results showed that the critical buckling strain (here referred to the strain on the inner arc of the bend at buckling) is a constant independent of the tube outer diameter, which is, however, in contradiction with the results from molecular dynamics simulations by Liew *et al.*[30] Recently, many novel numerical approaches have been proposed to investigate the mechanical behavior of relatively thick MWNT's, especially under bending.[7,14,32,33]

Compared to the numerical methods, analytical models usually give explicit solutions to the problems considered. The continuum shell model has been proven to be able to give a good approximation to the critical buckling strain of

SWNT's once the model parameters were properly chosen.[24,29,34,35] However, the single-shell model could not be directly applied to MWNT's due to the presence of interwall van der Waals interactions. To study the buckling behavior of MWNT's, Ru[36,37] developed a multishell model in which the interwall van der Waals interaction was modeled by a linear function of the jump in deflection of adjacent walls due to buckling. The model has been used to study the buckling of MWNT's under axial compression without and with the combination of radial pressure[37,38] and buckling of double-walled nanotubes (DWNT's) embedded in an elastic medium under axial compression[36] and torsion.[39] Postbuckling behavior of DWNT's under hydrostatic pressure was studied by Shen[40] with consideration of transverse shear deformations in the shell model. Curvature effects of van der Waals forces on the axial compressed buckling of a DWNT was investigated by Qian *et al.*[41] In a recent work by He *et al.*,[42] a new multishell model which takes the van der Waals interaction between any two layers into account was developed, and the effects of the tube radius and thickness on the critical buckling load of a MWNT were reevaluated. For the applicability and limitations of shell models, the reader is referred to the paper by Wang *et al.*[43] Another powerful tool to analytically investigate mechanical behavior of CNT's is the molecular mechanics model.[44,45] Chang *et al.*[35] obtained explicit solutions for the critical buckling strain of SWNT's via a molecular mechanics model in which the effect of tube chirality was taken into account. Despite these extensive analytical studies, no analytical solution has, however, so far been available for the critical buckling strain of MWNT's under bending.

In this paper, we present theoretical solutions to the critical buckling strain of MWNT's under both bending and axial compression using the molecular mechanics approach. We find that the buckling behavior of a very thick (solid) MWNT is quite different from that of a thin MWNT, which takes unconventional size effects on the critical buckling strain. The present solution can make efficient predictions compared with the existing results. Empirical explicit expressions for the critical buckling strains are also presented, and the critical buckling strain of a MWNT with arbitrary size can be simply calculated by these expressions.

II. MOLECULAR MECHANICS MODEL FOR CNT's

In the empirical force-field method of molecular mechanics, the total potential energy E_t can be expressed as a sum of several individual energy contributions:

$$E_t = U_\rho + U_\theta + U_\omega + U_\tau + U_{\mathrm{vdW}} + U_{\mathrm{es}}, \tag{1}$$

where U_ρ, U_θ, U_ω, and U_τ are energies associated with bond stretching, bond angle variation, bond inversion, and torsion, respectively; U_{vdW} and U_{es} are associated with van der Waals and electrostatic interactions,[44–46] respectively. Various functional forms may be used for these energy terms depending on the particular materials and loading conditions considered.

In some cases, such as the present problem of buckling of carbon nanotubes, it can be expected that only bond stretching (U_ρ), bond angle variation (U_θ), bond inversion (U_ω), and interlayer van der Waals (U_{vdW}) terms are significant in the total system potential energy. Hooke's law is often employed to characterize the interactions between bound atoms in the system, which has been proven to be efficient and accurate enough to describe the behavior of atoms under small deformation.[46] That is,

$$U_\rho = \sum \frac{1}{2} K_\rho (\mathrm{d}r)^2, \quad U_\theta = \sum \frac{1}{2} C_\theta (\mathrm{d}\theta)^2, \quad U_\omega = \sum \frac{1}{2} C_\omega (\beta)^2, \tag{2}$$

where $\mathrm{d}r$ is the bond elongation, $\mathrm{d}\theta$ the bond angle variance, and β the average inversion angle (whose definition can be found in Ref. 35). Force constants may be taken as $K_\rho = 742$ nN/nm, $C_\theta = 1.42$ nN nm (obtained by Chang and Gao[45] from physical data of graphite), and $C_\omega = 3.27$ nN nm (calculated by $24D_0$, where $D_0 = 0.85$ eV is the bending stiffness of graphene sheets[24]).

The van der Waals force between any two atoms can be well described by the Lennard-Jones (LJ) model.[47,48] Following Ru's multishell model,[36] in view of the linearized features of the infinitesimal buckling analysis, the total van der Waals force exerted on any atom due to all atoms of the interacting adjacent tube may be a linear function of the jump in deflection at the atomic position. This means

$$U_{\mathrm{vdW}} = \sum \frac{1}{2} K_{\mathrm{vdW}} (\mathrm{d}s)^2, \tag{3}$$

where $\mathrm{d}s$ is the jump in deflection at the atomic position. It should be noted that the value of K_{vdW} is dependent on the ratio of the diameter of the tube interacting with the atom. For example, He *et al.*[42] have clearly shown that the van der Waals force is dependent on the tube diameter and the change of the K_{vdW} value is higher than 10% due to the variation of tube diameter.

In fact, an atom interacts with not only the nearest-neighboring layers, but also the non-nearest-neighboring layers via van der Waals forces. It is no doubt that the model with consideration of the van der Waals interaction between any two layers may give a more accurate analysis of the buckling of MWNT's than the model accounting only for the van der Waals interaction from the nearest-neighboring layers. He *et al.*,[42] using a novel multishell model, have investigated the axial buckling of MWNT's with consideration of van der Waals interactions between any two layers. However, they showed that the van der Waals interaction coefficients for the two nonadjacent layers is at least 50 times lower than those for the two adjacent layers,[42] which means that the van der Waals interaction from the non-nearest-neighboring layers is not significant compared to that from the nearest-neighboring layers.

On the other hand, numerical results by Pantano *et al.*[15] have indicated that, even if the van der Waals strength is reduced to 50%, the change of the critical buckling strain (or load) of a nine-walled CNT is not more than 5%, and its initial buckling wavelength remains unchanged. The results actually imply that a small variation of the van der Waals interaction coefficients has little effect on the critical buck-

ling parameters of a MWNT. Hence it seems acceptable to ignore the van der Waals interaction from non-nearest-neighboring layers and the effect of tube diameter on K_{vdW} during the investigation of the critical buckling behavior of MWNT's, as in Ru's multishell model.[36] Such simplicity will slightly change the quantity of the critical buckling strain (or load) of a MWNT because of the reduction of the lateral constraint of individual tubes, but it is believed that it will not bring a qualitative change of the critical buckling behavior of a MWNT.

In this paper, similar to Ru's multishell model,[36] we only consider the van der Waals interactions from the nearest-neighboring layers and simply take $K_{\mathrm{vdW}}=K_v=1.62$ nN/nm, which is in fact the value for an atom interacting with a graphene sheet to which the distance from the atom is about 0.34 nm. Typical results from the present model will be compared with the corresponding ones from the model of He *et al.*,[42] as well as those from Ru's model,[36] to verify the model's efficiency (see Table II, where the maximum error is less than 4%).

In terms of Eqs. (2) and (3), the system energy of the present problem can be written as

$$E_t=\frac{1}{2}\sum_i\frac{1}{2}K_\rho\sum_{p=1}^{3}(\mathrm{d}r_{ip})^2+\sum_i\frac{1}{2}C_\theta\sum_{p=1}^{3}(\mathrm{d}\theta_{ip})^2+\sum_i\frac{1}{2}C_\omega(\beta)^2+\frac{1}{2}\sum_i\frac{1}{2}K_v[(\mathrm{d}\omega_i^+)^2+(\mathrm{d}\omega_i^-)^2], \tag{4}$$

where the coefficient 1/2 of the first and fourth terms is to ensure that the energies are considered only once; $p=1-3$ in the first and second terms is due to the fact that there are three bond lengths and three bond angles associated with atom i; w_i is the radial displacement of atom i, and $\mathrm{d}w^+$ ($\mathrm{d}w^-$) represents the jump in the deflection between the wall on which atom i located and its inner (outer) adjacent wall. It should be noted that $\mathrm{d}w^+$ ($\mathrm{d}w^-$) should be set to be zero for the innermost (outermost) wall.

The critical buckling strain of an axial compressive or bending CNT will be determined by an energy approach as follows. The system free energy Π, which is the difference of system strain energies before ($\mathrm{d}E$) and after buckling (ΔE), can be related to the buckling strain and buckling mode. The equilibrium equation in the normal direction for each atom is then obtained via the requirement of a minimum of the system free energy. The nontrivial solution of the buckling deflections needs the determinant of the coefficient matrix of the equilibrium equations being zero, which consequently leads to an N-order equation for the buckling strain whose minimum value gives the critical buckling strain.

III. BUCKLING OF SWNT's UNDER AXIAL COMPRESSION

A single-walled carbon nanotube, which can be viewed as a graphene sheet rolled into a tube, is usually indexed by a pair of integers (n_1,n_2) to represent its helicity.[49] A molecular mechanics model for axisymmetrical buckling of SWNT's (i.e., which deform into a ring pattern at the critical buckling) has been established by Chang *et al.*[35] In this section, we briefly outline the main results from the model and then extend the model to MWNT's in the subsequent sections.

Let ε be the compressive strain and ε_0 the buckling strain, and assume that a (n,n) SWNT (often referred to an armchair tube) buckles into a ring pattern which can be described by a cosine function. The system free energy can be written as[35]

$$\Pi=\mathrm{d}E-\Delta E, \tag{5}$$

where $\mathrm{d}E$ and ΔE can be related to the compressive strain and buckling mode via Eq. (4).[35] The extremum condition of Π leads to

$$\frac{\partial\Pi}{\partial\zeta_i}=\frac{\partial(\mathrm{d}E-\Delta E)}{\partial\zeta_i}=0, \tag{6}$$

where ζ_i is the radial displacement of the atom i. Equation (6) consequently gives the equilibrium equation for each atom as[35]

$$(f_1+g_1\varepsilon_0)z_1=0, \tag{7}$$

where z_1 is the buckling amplitude.

Nontrivial solution of the buckling amplitude leads to the characteristic equation[35]

$$f_1+g_1\varepsilon_0=0. \tag{8}$$

The parameters f_1 and g_1 for armchair tubes in Eqs. (7) and (8) are calculated by[35]

$$f_1=\frac{C_\omega}{9r_0^2}p_T+\frac{K_\rho r_0^2}{64R^2}p_Y-\frac{2C_\theta\phi_A}{\sqrt{3}r_0^2}p_G, \tag{9}$$

$$g_1=\frac{3K_\rho}{3+\lambda_A(K_\rho r_0^2/C_\theta)}p_D+\frac{2C_\theta}{\sqrt{3}r_0^2}[\kappa_{A1}p_G+\kappa_{A3}p_S], \tag{10}$$

where R is the tube radius and r_0 is the reference C-C bond length. The other parameters are[35]

$$p_T=16\sin^4(\xi/2), \tag{11}$$

$$p_S=4[4\sin^4(\xi/2)-\sin^2(\xi/2)], \tag{12}$$

$$p_G=4\sin^2(\xi/2), \tag{13}$$

$$p_D=-4\sin^2(\xi/2), \tag{14}$$

$$p_Y=2[17+\cos\xi], \tag{15}$$

$$\lambda_A=\frac{7-\cos(\pi/n)}{34+2\cos(\pi/n)}, \tag{16}$$

$$\kappa_{A1}=\frac{3\sqrt{2}\lambda_A(K_\rho r_0^2/C_\theta)}{3+\lambda_A(K_\rho r_0^2/C_\theta)}\frac{1}{\sqrt{7-\cos(\pi/n)}}\cos\frac{\pi}{2n}, \tag{17}$$

$$\kappa_{A3}=\frac{2\sqrt{3}\lambda_A(K_\rho r_0^2/C_\theta)}{3+\lambda_A(K_\rho r_0^2/C_\theta)}, \tag{18}$$

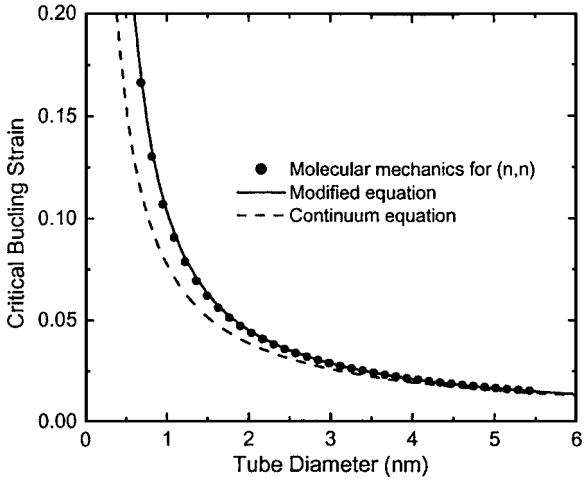

FIG. 1. Critical buckling strain for axial compressed SWNT's from different methods.

$$\phi_A = \frac{\pi}{3} - \arccos\left(\frac{1}{2}\cos\frac{\pi}{2n}\right), \tag{19}$$

$$\xi = \frac{\sqrt{3}m\pi r_0}{2L}, \tag{20}$$

where L is the tube length and m the number of half waves in the axial direction. The critical buckling strain ε_c is determined as the minimum value of the buckling strain ε_0 in Eq. (8). For more details of the procedure, the reader is referred to the paper by Chang *et al.*[35]

Here we should emphasize that an equation from the continuum shell theory would underestimate the critical buckling strain of a SWNT especially when the tube diameter is small (Fig. 1).[35] The reason is partly due to the size-dependent elastic modulus of SWNT's and partly due to the fact that a small SWNT may behave as a thick tube rather than a thin one (because all SWNT's have the same "thickness" in the concepts of continuum theory).

Based on a detailed analysis on the data shown in Fig. 1, we find that the critical buckling strain for an axial compressed (n,n) SWNT can be well approximated by an empirical equation

$$\varepsilon_c = \frac{4}{d}\sqrt{\frac{D_0}{Et}}\left(1+\frac{t}{d}\right); \tag{21}$$

i.e., the equation obtained from continuum mechanics is modified by multiplying a factor of $(1+t/d)$. Here $t=0.339$ nm is the effective wall thickness, d the diameter, D_0 the bending stiffness, and Et the in-plane stiffness of the SWNT. Comparisons of the results from the molecular mechanics model with the continuum equation and the modified equation are shown in Fig. 1, where $D_0=0.85$ eV and $Et=360$ J/m^2 as obtained by Yakobson *et al.*[24] are used.

IV. BUCKLING OF MWNT's UNDER AXIAL COMPRESSION

For an N-walled CNT, although a diamondlike mode can be observed at the final buckling stage, MD simulations have shown that the initial buckling mode of a MWNT is in a ring pattern.[30] Thus the above approach is particular useful to determine the critical buckling strain of MWNT's. The system free energy for a MWNT is the summation of the intratube energies, $\mathrm{d}E_{\mathrm{intra}}-\Delta E_{\mathrm{intra}}$, and the intertube van der Waals interactions, $\mathrm{d}E_{\mathrm{inter}}-\Delta E_{\mathrm{inter}}$,

$$\begin{aligned}\Pi &= (\mathrm{d}E_{\mathrm{intra}} - \Delta E_{\mathrm{intra}}) + (\mathrm{d}E_{\mathrm{inter}} - \Delta E_{\mathrm{inter}}) \\ &= \sum_{k=1}^{N}(\mathrm{d}E^{(k)} - \Delta E^{(k)}) + \sum_{k=1}^{N-1}(\mathrm{d}E_{\mathrm{vdW}}^{(k,k+1)} - \Delta E_{\mathrm{vdW}}^{(k,k+1)}),\end{aligned} \tag{22}$$

where the superscript k is the wall index numbered from the outermost tube to the innermost tube, $\mathrm{d}E^{(k)}$ and $\Delta E^{(k)}$ are the intratube strain energies for the kth wall of the MWNT, and $\mathrm{d}E_{\mathrm{vdW}}^{(k,k+1)}$ and $\Delta E_{\mathrm{vdW}}^{(k,k+1)}$ represent the intertube van der Waals interaction potentials between the kth and $(k+1)$th individual tubes.

We seek the radial displacement of atom i located on the kth wall due to axisymmetric buckling as

$$\zeta_i = \zeta^{(k)}(x_i) = z^{(k)}\cos\frac{m\pi x_i}{L} + z_0^{(k)}, \tag{23}$$

where L is the length of nanotube, m the half wave numbers along the tube axis direction, x_i the longitudinal coordinate of atom i, and $z^{(k)}$ the bucking amplitude and $z_0^{(k)}$ the radial extension of the nanotube before buckling.

The extremum condition of Π leads to

$$\begin{aligned}\frac{\partial\Pi}{\partial\zeta_i} = \frac{\partial(\mathrm{d}E^{(k)} - \Delta E^{(k)})}{\partial\zeta_i} + \frac{K_{\mathrm{vdW}}}{2}\frac{\partial}{\partial\zeta_i}\{[\zeta^{(k+1)}(x_i) - \zeta^{(k)}(x_i)]^2 \\ + [\zeta^{(k)}(x_i) - \zeta^{(k-1)}(x_i)]^2\} = 0.\end{aligned} \tag{24}$$

Here we should note that for an N-walled nanotube, $\zeta^{(N+1)}(x)=\zeta^{(0)}(x)=0$. Equation (24) in fact gives the radial equilibrium equation of atom i. When the van der Waals interaction is absent, Eq. (24) can be simplified to Eq. (6) for a SWNT. With use of Eq. (23), to keep Eq. (24) a permanent equation, it needs two constraint equations. One of them may be used to calculate $z_0^{(k)}$ and will not be discussed here because it has no contributions to the problem we considered. The other for $z^{(k)}$ can be written as

$$(f_k + g_k\varepsilon_0)z^{(k)} - K_v(z^{(k+1)} - 2z^{(k)} + z^{(k-1)}) = 0, \tag{25}$$

with $z^{(N+1)}=z^{(0)}=0$ for an N-walled nanotube. Comparing Eq. (25) to Eq. (7), as can be expected, the characteristic equations for a MWNT are coupled by the intertube van der Waals interactions. The parameters f_k and g_k for armchair tubes are calculated by

$$f_k = \frac{C_\omega}{9r_0^2}p_T + \frac{K_\rho r_0^2}{64R_k^2}p_Y - \frac{2C_0\phi_A^{(k)}}{\sqrt{3}r_0^2}p_G, \tag{26}$$

$$g_k = \frac{3K_\rho}{3+\lambda_A^{(k)}(K_\rho r_0^2/C_0)} p_D + \frac{2C_\theta}{\sqrt{3}r_0^2}[\kappa_{A1}^{(k)} p_G + \kappa_{A3}^{(k)} p_S], \quad (27)$$

where the superscript k indicates that the parameters, which can be calculated by Eqs. (11)–(20), are related to the kth wall.

We rewrite Eq. (25) in a matrix form as

$$[\mathbf{M}]\{\mathbf{z}\} = 0, \quad (28)$$

where the coefficient matrix

$$[\mathbf{M}] = \begin{bmatrix} f_1 + g_1\varepsilon_0 + K_v & -K_v & 0 & \cdots & 0 & 0 \\ -K_v & f_2 + g_2\varepsilon_0 + 2K_v & -K_v & \cdots & 0 & 0 \\ 0 & -K_v & f_3 + g_3\varepsilon_0 + 2K_v & \cdots & 0 & 0 \\ \cdots & \cdots & \cdots & \cdots & \cdots & \cdots \\ 0 & 0 & 0 & \cdots & f_{N-1} + g_{N-1}\varepsilon_0 + 2K_v & -K_v \\ 0 & 0 & 0 & \cdots & -K_v & f_N + g_N\varepsilon_0 + K_v \end{bmatrix}, \quad (29)$$

and the vector $\mathbf{z}$ represents the buckling amplitude of each individual tube:

$$\{\mathbf{z}\} = \{z^{(1)}, z^{(2)} z^{(3)}, \ldots, z^{(N)}\}^T. \quad (30)$$

Nontrivial solution of $\mathbf{z}$ need the determinant of matrix $\mathbf{M}$ to be zero—i.e.,

$$\mathrm{Det}[\mathbf{M}] = 0, \quad (31)$$

which consequently yields an N-order equation of ε_0. The buckling strain ε_0 corresponding to a given buckling mode for any N-walled tubes, in principle, can be obtained from such an N-order equation, and the critical buckling strain ε_c should be the minimum value of ε_0. The buckling wavelength is then calculated by ξ associated with ε_c:

$$l = \sqrt{3}\pi r_0/\xi, \quad (32)$$

where ξ is defined in Eq. (20).

Because the tube chirality has no essential effect on the critical buckling strain of CNT's,[35] the present discussions are focused only on the buckling of armchair tubes. Without loss of generality, only the buckling of MWNT's that are constructed of nested $(5n,5n)$ tubes is discussed in this paper.

V. BUCKLING OF MWNT's UNDER BENDING

The critical buckling strain of a bent MWNT can be obtained by applying the above approach to the local compressive strain, as suggested by Yakobson *et al.*[24] in calculating the critical buckling strain of a SWNT, only if the proportional distribution of the compressive strain along the radial direction in the bending plane is taken into account. A similar analysis leads to the same characteristic equations such as those shown in Sec. III, except that Eq. (27) should be modified as

$$g_k = \mu\left(\frac{3K_\rho}{3+\lambda_A^{(k)}(K_\rho r_0^2/C_\theta)} p_D + \frac{2C_\theta}{\sqrt{3}r_0^2}[\kappa_{A1}^{(k)} p_G + \kappa_{A3}^{(k)} p_S]\right), \quad (33)$$

in which

$$\mu = \begin{cases} 1 & \text{under axial compression,} \\ d_k/d_o & \text{under bending,} \end{cases} \quad (34)$$

where d_k is the diameter of the kth wall and $d_o = d_1$ the diameter of the outermost wall.

VI. DISCUSSIONS OF THE RESULTS

The critical buckling of a MWNT under axial compression or bending can be determined from Eq. (31). For any given buckling mode parameter ξ [which is defined in Eq. (20)], there exist N solutions of Eq. (31). With the variation of ξ from 0 to $\pi/2$, there is a minimum value among these solutions which is the critical buckling strain of the problem.

A. Classification of MWNT's

Once the critical buckling strain of the problem is determined from Eq. (31), one can substitute the value of ε_c as well as the corresponding ξ into Eq. (28) to obtain an equation set about the buckling amplitude of each individual tube. The equation set cannot be directly solve because the determination of the coefficient matrix $\mathbf{M}$ is zero [see Eq. (31), which is used to determine ε_c]. It is, nevertheless, easy to find that the relative value of the initial buckling amplitude $z^{(k)}/z^{(1)}$ could be determined from Eq. (28) as

$$\bar{z}^{(1)} = 1,$$

$$\bar{z}^{(2)} = \frac{f_1 + g_1\varepsilon_c}{K_v} + 1,$$

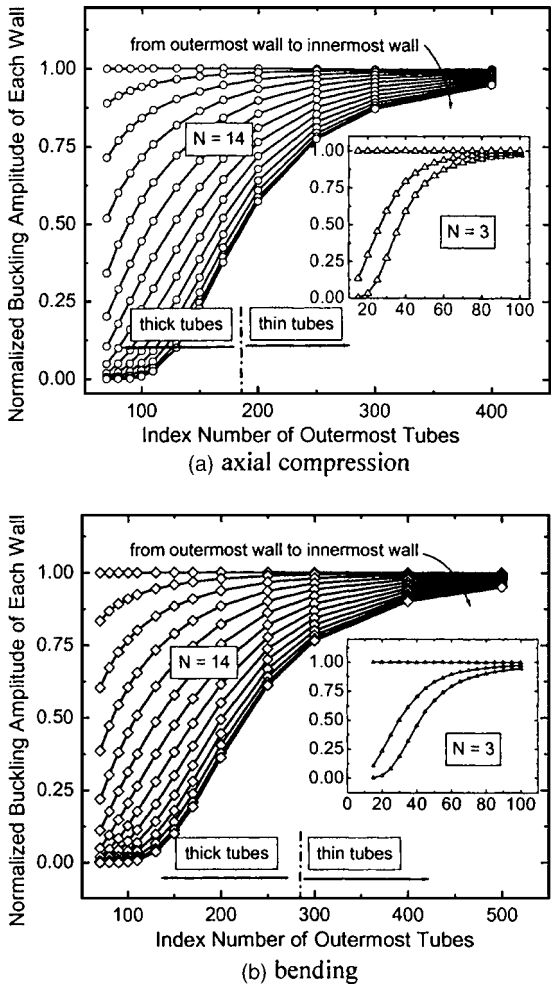

FIG. 2. Normalized initial buckling amplitudes of MWNT's versus index number of outermost tubes under (a) axial compression and (b) bending.

$$\bar{z}^{(k)} = \left(\frac{f_{k-1} + g_{k-1}\varepsilon_c}{K_v} + 1 \right) \bar{z}^{(k-1)} - \bar{z}^{(k-2)} \quad (\text{for } k > 2), \tag{35}$$

where $\bar{z}^{(k)} = z^{(k)}/z^{(1)}$ is the normalized initial buckling amplitude.

Figures 2(a) and 2(b) show the normalized initial buckling amplitudes of individual tubes of 14-walled and 3-walled CNT's under axial compression and bending, respectively. It is seen clearly that the buckling modes of thin and thick tubes are quite different. The buckling amplitudes of all individual tubes in very thin tubes are nearly the same, while in thick tubes, the buckling amplitude of the outermost tube is much larger than that of the innermost one. In particular, we find that the buckling amplitudes of some inner individual tubes of a very thick MWNT are almost zero. For example, the buckling amplitude of the outer layer is about 10 times larger than that of the middle layer and about 400 times larger than that of the inner layer of a bent 3-walled $(5n,5n)_{n=1-3}$ tube [Fig. 2(b)]. In other words, only part of the outer walls buckles first while the rest inner part remains stable. This finding gives a theoretical confirmation of the recent observation in molecular dynamics simulations of CNT buckling by Liew *et al.*[30] They found that only the outer layer of a 3-walled $(5n,5n)_{n=1-3}$ tube buckles first at $\varepsilon = 0.0484$, while the middle and inner layers remain stable. This special buckling mode has been denoted as mode-I buckling, while the buckling mode of all individual tubes buckling together is named mode-II buckling in our previous paper.[35] A *solid* (very thick) MWNT may now be defined as the MWNT corresponding to mode-I buckling.

According to our further analysis (results will be shown in the following sections, especially in Fig. 7), we defines *thin* and *thick* MWNT's as that shown in Table I. However, it should be noted that the transition point of thin-to-thick tubes is dependent upon the load conditions added to the MWNT's.

B. Critical buckling strain of solid MWNT's

The critical buckling strain of $(5n,5n)_{n=1-N}$ MWNT's (which can be viewed as solid MWNT's when $N>2$) is shown in Fig. 3. We can see that the critical buckling strain decreases with increasing layers of the MWNT (i.e., increasing outer diameter of the MWNT) under both load conditions. This phenomenon is quite different from that of a continuum shell due to the fact that the intertube van der Waals interaction is much weaker than the intratube binding interaction, which makes the MWNT's highly anisotropic. Further analysis shows that the critical buckling strain for a solid MWNT can be well represented by $0.0985\ \text{nm}/d_o$ for axial compression and $0.111\ \text{nm}/(d_o+t)$ for bending, where d_o is the outer diameter and $t=0.339$ nm is the interlayer spacing of the MWNT. Namely, the critical buckling strain of an axial compressed solid MWNT is in reverse proportion to its outer diameter d_o, while the critical buckling strain of a bent solid MWNT is in reverse proportion to (d_o+t).

Some existing results from molecular dynamics simulations,[30] the modified finite-element method,[6,15] quasicontinuum mechanics calculations,[14] and an experimental

TABLE I. Classification of MWNT's under axial compression and bending.

	Thin MWNT's		Thick MWNT's			
			General		Solid (very thick)	
	Compression	Bending	Compression	Bending	Compression	Bending
d_i/d_o	>0.62	>0.75	<0.62	<0.75	<0.35	<0.41

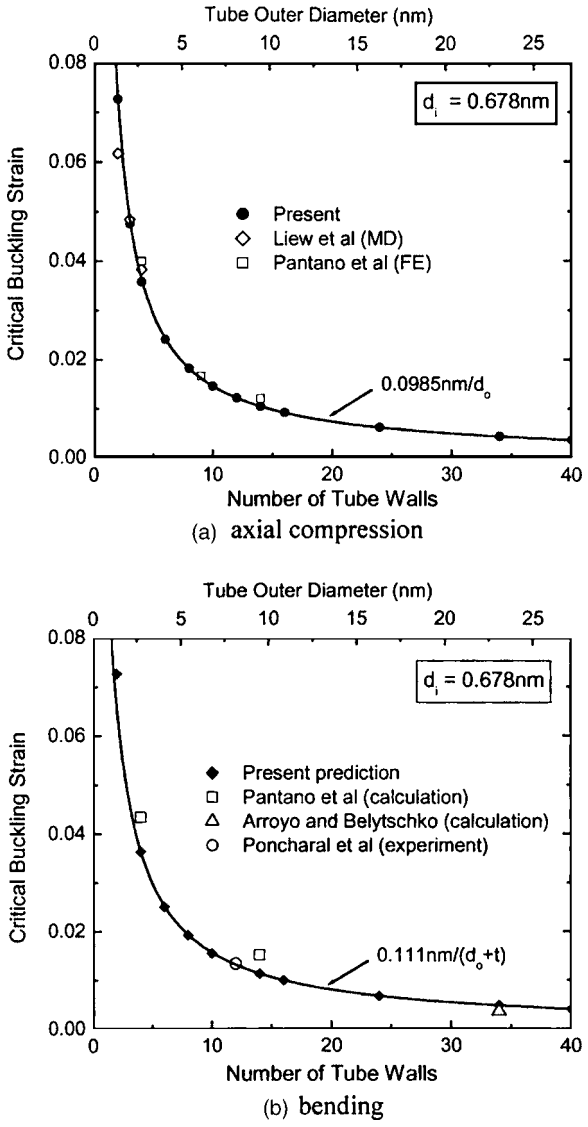

FIG. 3. Critical buckling strain of solid MWNT's versus number of tube walls (tube outer diameter) under (a) axial compression and (b) bending.

test[9] are also shown in the figures for comparison. The agreement is found to be very good in both load conditions.

C. Size effects on the critical buckling strain of MWNT's

In this section, the size effects on the critical buckling strain of the MWNT will be discussed in detail. There are three ways to make a thin MWNT into a thicker one: (1) inserting inner tubes, (2) wrapping outer tubes, and (3) inserting and wrapping simultaneously. As the present analysis is confined to the MWNT's constructed of nested $(5n,5n)$ tubes, so the difference of the index number of every two neighboring individual tubes is kept 5 while inserting and wrapping.

1. Inserting effects

Figure 4 shows how the critical buckling strain varies

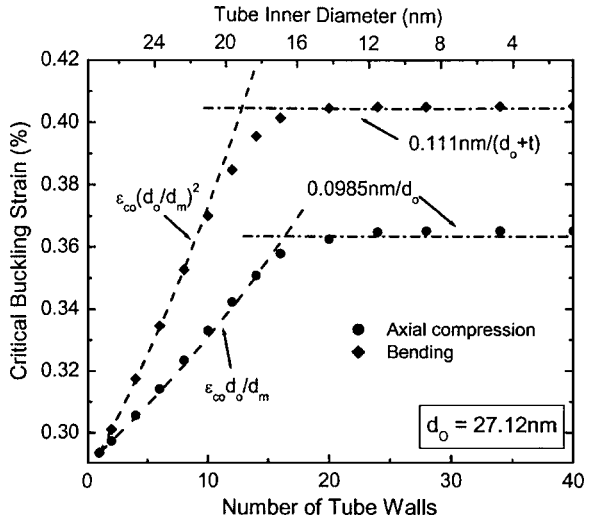

FIG. 4. Thickness effects on the critical buckling strain of MWNT's when the tube outer diameter is kept constant.

with the increasing number of tube walls in the case of the tube outer diameter d_o remaining unchanged. It is seen that the critical buckling strain for thinner MWNT's can be increased by inserting inner tubes. However, with the tube thickness increasing to some critical value (which indicates the thin-to-thick transition), the critical buckling strain becomes stable. The insensitivity to further insertion of the critical buckling strain of a thick MWNT can be explained by the phenomenon we observed in Sec. IV A; i.e., the inserted inner tubes may not be involved into critical buckling of a very thick (solid) MWNT. We note here again that the points of thin-to-thick transition may shift with loading conditions.

For an axial compressive thin MWNT ($N<16$ in Fig. 4), its critical buckling strain can be well represented by $\varepsilon_{co}d_o/d_m$, where ε_{co} is the critical buckling strain for a SWNT with the same diameter as the outer diameter of the MWNT and d_m the mean diameter [i.e., $(d_i+d_o)/2$] of the MWNT. The value of $\varepsilon_{co}d_o/d_m$ is in fact approximately equal to the critical buckling strain of a SWNT with a diameter of d_m (for convenience, we denote it as ε_{cm}). This means that the critical buckling strain of an axial compressed thin MWNT can be approximated by that of a SWNT with the diameter equal to the mean diameter of the MWNT. This finding agrees with that given by Ru using a multishell model.[37] For an axial compressive thick MWNT, because it is insensitive to the tube inner diameter, the critical buckling strain can be approximated by the above mentioned fitting function for solid tubes with a (5,5) tube as the innermost tube, 0.0985 nm$/d_o$.

With respect to bent MWNT's, the critical buckling strain of a thick tube ($N>12$ in Fig. 4) is also insensitive to its inner diameter and can similarly be fitted by 0.111 nm$/(d_o+t)$, while the critical buckling strain of a thin tube is approximately equal to $\varepsilon_{co}(d_o/d_m)^2$. Thus we have the critical buckling *curvature* $\kappa_c=\varepsilon_c/R_o=(\varepsilon_{co}d_o/d_m)/R_m\approx\varepsilon_{cm}/R_m=\kappa_{cm}$. This means that the critical buckling curvature of a bent thin MWNT can be approximated by that of a SWNT with the diameter equal to the mean diameter of the MWNT.

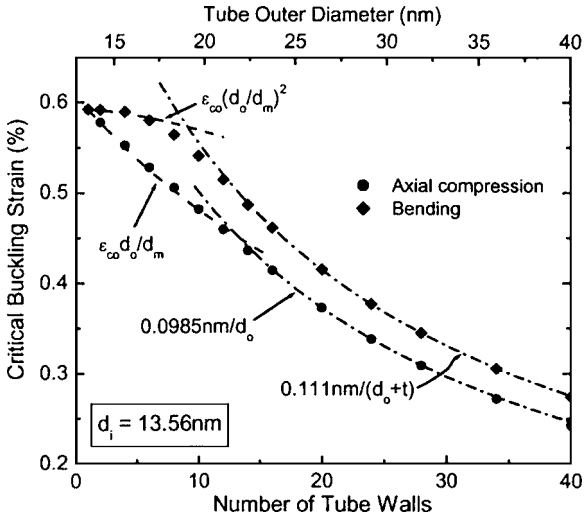

FIG. 5. Thickness effects on the critical buckling strain of MWNT's when the tube inner diameter is kept constant.

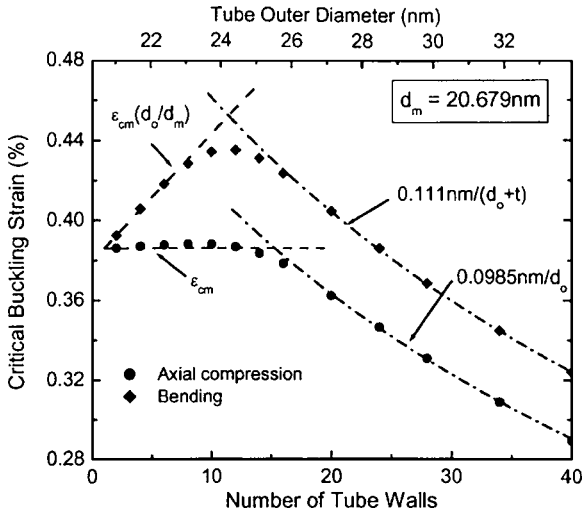

FIG. 6. Thickness effects on the critical buckling strain of MWNT's when the tube mean diameter is kept constant.

This is a very important conclusion which can be used to estimate the critical buckling condition of a bent thin MWNT.

2. Wrapping effects

In Fig. 5 we show wrapping effect on the critical buckling strain where the tube inner diameter is remained as that of a (100,100) SWNT—i.e., $d_i=d_{(100,100)}$. The same trend as shown in Fig. 3 can be seen in Fig. 5; i.e., wrapping more individual tubes will decrease the buckling strain of a MWNT. Compared with empirical expressions to thin and thick tubes, we can find clearly the thin-to-thick transition points under both loading conditions.

3. Inserting and wrapping

It means that the tube mean diameter remains unchanged if the same number of individual SWNTs is wrapped on as is inserted in an existing MWNT. How the critical buckling strain varies with the tube thickness in this case is dependent on the competition of the effect resulting from the inserting tube and the wrapping tube. We can see from Fig. 6 that, with increasing tube thickness, the critical buckling strain of a thin MWNT remains almost constant under axial compression, but it significantly increases under bending. This implies that the inserting effect is almost equal to the wrapping effect for a thin MWNT under axial compression, while for a bent thin MWNT, the inserting effect is much stronger than the wrapping effect. As can be expected, the critical buckling strain of a thick MWNT under both loading conditions will be decreased by the wrapping tube as the inserting tube has almost no effect on it (because it may not be involved in the buckling). Again, the effective predictions of the fitting functions are shown in Fig. 6, where ε_{cm} is the critical buckling strain of a SWNT with a diameter equal to the mean diameter of the MWNT's.

Finally, we show in Table II the comparison of the present results with some other existing results for both thin and thick tubes besides those presented in Fig. 3. Good agreement is found again (with errors less than 4%).

D. Correlation of the critical buckling strain

Shown in Fig. 7 is the normalized critical buckling strain versus tube thickness parameter Nt/d_m. The critical buckling strain of each tube is normalized by that of the corresponding solid MWNT [whose innermost tube is (5, 5)] with the same outermost diameter. Surprisingly, we find that all data points

TABLE II. Comparison of the present predictions of the critical buckling strain for MWNT's under axial compression with existing results.

	Thin MWNT's					Thick MWNT's				
d_i (nm)	17.36	36.34	11.87	11.87	11.87	11.87	5.70	13.28	1.36	2.71
d_o (nm)	20.07	41.08	12.20	13.22	14.92	17.30	10.44	23.46	6.10	4.75
N	5	8	2	5	10	17	8	16	8	4
Previous (%)	0.423[a]	0.206[a]	0.322[b]	0.309[b]	0.290[b]	0.264[b]	0.935[a]	0.421[a]	1.54[a]	~2[c]
Present (%)	0.428	0.206	0.331	0.318	0.299	0.273	0.943	0.419	1.61	2.06

[a]Wang *et al.* (Ref. 38) from a multishell model in which only the vdW interaction between adjacent two layers is considered.
[b]He *et al.* (Ref. 42) using a multishell model in which the vdW interaction between any two layers is considered.
[c]Srivastava and Barnard (Ref. 25) by molecular dynamics simulations.

fall onto a unique curve in each loading condition, which means the critical buckling strain of a MWNT with arbitrary size can be described by a unified function in each loading condition.

We can find clearly from Fig. 7 that the maximum enhancement of the critical buckling strain of a SWNT (or MWNT) by inserting inner tubes (while remaining interwall spacing as 0.339 nm) is about 26% under axial compression and 42% under bending, respectively. The thin-to-thick transition points can be seen clearly also, which indeed gave the definitions of the thin and thick tubes under both load conditions as shown in Table I.

The two curves shown in Fig. 7 can be well fitted by

$$\bar{\varepsilon}_c = 1 - \frac{\delta}{1+\delta} f(\tau), \tag{36}$$

where the thickness parameter τ equals to Nt/d_m and the maximum inserting effect δ and switching function $f(\tau)$ are given by

$$\begin{cases} \delta = 0.26,\ f(\tau) = (1+\tau)^{-1}(1-\tau)^{3/(1-\tau)^3} & \text{under axial compression,} \\ \delta = 0.42,\ f(\tau) = (1+\tau)^{-1}(1-\tau)^{4/(1-\tau)^4} & \text{under bending.} \end{cases} \tag{37}$$

Together with the two fitting functions shown in Fig. 3 for the critical buckling strain of a solid MWNT under axial compression and bending, Eqs. (36) and (37) could give the approximate critical buckling strain of a MWNT with arbitrary size.

E. Initial buckling wavelength of MWNT's

The initial buckling wavelength, which is an important parameter in description of the buckling deformation of MWNT's, can be determined by Eq. (32) in which ξ is associated with the critical buckling strain ε_c. Shown in Fig. 8 is the initial buckling wavelength versus $(R_o h)^{1/2}$ for two series of MWNT's with constant $d_i = d_{(5,5)}$ and constant $d_o = d_{(200,200)}$, respectively, where R_o are the outer radius of the MWNT and $h = Nt$. It is shown that the initial buckling wavelength for axial compression is approximately the same as that for bending. Therefore, we will not distinguish them in the following discussion. The results for MWNT's with constant $d_i = d_{(5,5)}$ given by Pantano *et al.*[6] from a modified finite-element (FE) method are also shown in the figure for comparison and good agreement can be found (note here we take $t = 0.339$ nm other than 0.075 nm used in their plot).

To our surprise, the present results indicate that the initial buckling wavelength is weakly dependent upon the tube thickness (see the curve for MWNT's with constant $d_o = d_{(200,200)}$). This important finding seems quite different from the conclusions from single-shell theory.

Thin-shell theory predicts that the initial buckling wavelength for a cylindrical shell under axial compression can be written as[34,50]

$$l = 2\pi \left(\frac{D}{Eh}\right)^{1/4} \sqrt{R_o} = \frac{2\pi}{12(1-\nu^2)} \sqrt{R_o h}, \tag{38}$$

where $D = Eh^3/12(1-\nu^2)$ is the bending stiffness, E the elastic modulus, and ν the Poisson ratio. A ratio of $l/(R_o h)^{1/2}$ is found to be 3.4 if the Poisson ratio is taken as 0.19. The

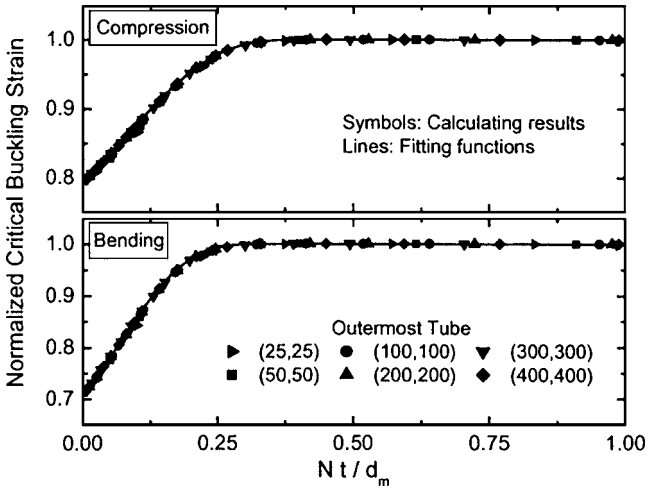

FIG. 7. Correlation of the critical buckling strain of MWNT's with arbitrary size.

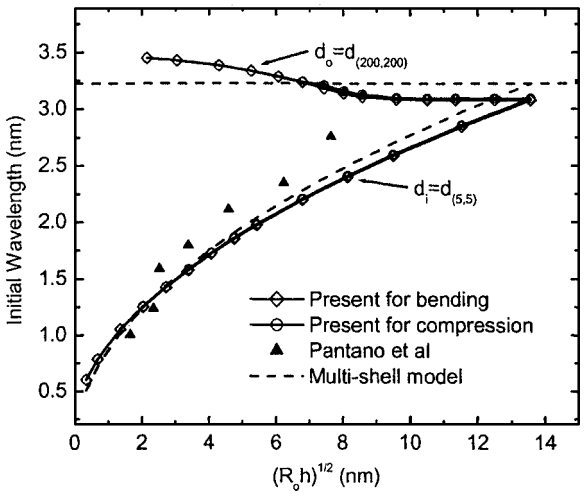

FIG. 8. Comparison of predictions from different approaches for the initial buckling wavelength of MWNT's.

experimental investigation by Bower *et al.*[23] showed a similar trend of the buckling wavelength in proportion to $(R_o h)^{1/2}$, but with a ratio of about 1. The difference was attributed to two facts. First, the MWNT's observed in the experiment are thick tubes.[23] Second, MWNT's possess a multiwalled structure other than a single shell.[7] Both of these two facts would make the single-shell model unsuitable to be directly applied to MWNT's. However, it is proven that a multishell model is suitable for studying the buckling of a MWNT.[37] In the study on the axial buckling of MWNT, Ru[37] has concluded that the effective bending modulus of a thin MWNT (which is defined by the ratio of the inner-to-outer diameter larger than 0.75 in their work) is approximately N times of the SWNT (which is $25N^2$ times lower than that predicted by the single-shell model). This means that the initial buckling wavelength of a MWNT could not be correctly predicted by Eq. (38), but could be calculated by the effective bending modulus

$$l = 2\pi\left(\frac{D}{Eh}\right)^{1/4}\sqrt{R_o} = 2\pi\left(\frac{ND_0}{ENt}\right)^{1/4}\sqrt{R_o} = 2\pi\left(\frac{D_0}{Et}\right)^{1/4}\sqrt{R_o}$$
$$\approx \sqrt{0.77\ \text{nm}\, R_o}, \tag{39}$$

where $D_0 = 0.85$ eV and $Et = 360\ \text{J/m}^2$ are used.[24] The results from Eq. (39) are also shown in Fig. 8. We can see that the prediction of the multishell model is very close to the present results even for thick MWNT's. The right-hand side of Eq. (39) is actually equal to the initial buckling wavelength of a SWNT with a radius of R_o. This means that the initial buckling wavelength of a MWNT is approximately equal to the initial buckling wavelength of a SWNT with the same diameter as the MWNT.

It should be pointed out that the present model only predicts the *initial* buckling wavelength, while an experiment almost always measures the *final* buckling wavelength far away from the critical buckling state. Numerical simulations have shown that the final buckling wavelength is much larger than the initial buckling wavelength.[6] Therefore, it is not suitable to directly compare the present results with the experimental data and there need further analytic studies on the post-buckling of MWNT's.

VII. CONCLUSIONS

In summary, we present theoretical solutions to calculate the critical buckling strain of MWNT's under axial compression and bending. The results indicate that the initial buckling mode of a very thick tube is quite different from that of a thin tube. In a very thick MWNT, only part of outer layers buckles first while the remaining inner part remains stable, while in a relatively thin MWNT, all individual tubes buckle simultaneously. Such a difference in the initial buckling mode takes unconventional size effects on the critical buckling strain (or curvature) of MWNT's. For a thin MWNT under bending (axial compression), the critical buckling curvature (strain) can be approximated by that of a SWNT with a diameter same as the mean diameter of the MWNT. However, the critical buckling strain of a thick MWNT is insensitive to its thickness and only a function of its outer diameter under both loading conditions. We also show the wrapping and inserting effects on the critical buckling strain of MWNT's. Wrapping more outer individual tubes will decrease the critical buckling strain of an existing MWNT. Inserting more inner individual tubes may increase the critical buckling strain of a thin MWNT, but cannot increase the critical buckling strain of thick tube. The maximum enhancement of insertion is shown to be not more than 26% under axial compression and 42% under bending, respectively. When normalized by the corresponding value for a very thick (solid) MWNT with the same outer diameter, the critical buckling strain of the MWNT's with arbitrary size would fall onto a unique curve in each load condition. This finding is very helpful in predicting the critical buckling strain of the MWNT's. The size effects on the initial buckling wavelength are also investigated. It is shown that the initial buckling wavelength is weakly dependent on the thickness of the MWNT and approximately equal to the initial buckling wavelength of a SWNT with the same diameter as the MWNT.

The present results are in good agreement with those given by molecular dynamics simulations and experimental observation. Comparisons with the existing results from continuum mechanics models, such as the modified finite-element method and the multishell models, show that a continuum mechanics model can give quite reasonable description to the buckling behavior of MWNT's if the key features of the MWNT's were well captured and the physical parameters were properly defined in the model.

ACKNOWLEDGMENTS

We gratefully acknowledge the financial support from the National Natural Science Foundation of China, Shanghai Rising-Star Program, Shanghai Postdoctoral Science Fund, Shanghai Leading Academic Discipline Project (Y0103), Development Fund of Shanghai Committee of Education, and Key Project of Shanghai Committee of Science and Technology (04JC14034).

*Corresponding author. Electronic address: tchang@staff.shu.edu.cn

[1] M. S. Dresselhaus, G. Dresselhaus, and P. C. Eklund, *Science of Fullerenes and Carbon Nanotubes* (Academic Press, San Diego, 1996).

[2] B. I. Yakobson and R. E. Smalley, Am. Sci. **85**, 324 (1997).

[3] R. E. Smalley and B. I. Yakobson, Solid State Commun. **107**, 597 (1998).

[4] D. Qian, G. J. Wagner, W. K. Liu, M. F. Yu, and R. S. Rouff, Appl. Mech. Rev. **55**, 495 (2002).

[5] H. M. Cheng, *Carbon Nanotubes: Synthesis, Microstructure, Properties and Applications* (Chemical Industry Press, Beijing, China, 2002).
[6] A. Pantano, M. C. Boyce, and D. M. Parks, Phys. Rev. Lett. **91**, 145504 (2003).
[7] A. Pantano, D. M. Parks, and M. C. Boyce, J. Mech. Phys. Solids **52**, 789 (2004).
[8] M. R. Falvo, G. J. Clary, R. M. Taylor, V. Chi, F. P. Brooks, Jr., S. Washburn, and R. Superfine, Nature (London) **389**, 582 (1997).
[9] P. Poncharal, Z. L. Wang, D. Ugarte, and W. A. de Heer, Science **283**, 1513 (1999).
[10] E. W. Wong, P. E. Sheehan, and C. M. Lieber, Science **277**, 1971 (1997).
[11] M. F. Yu, O. Lourie, M. J. Dyer, K. Moloni, T. F. Kelly, and R. S. Ruoff, Science **287**, 63 (2000).
[12] J. Z. Liu, Q. S. Zheng, and Q. Jiang, Phys. Rev. Lett. **86**, 4843 (2001).
[13] J. Z. Liu, Q. S. Zheng, and Q. Jiang, Phys. Rev. B **67**, 075414 (2003).
[14] M. Arroyo and T. Belytschko, Phys. Rev. Lett. **91**, 215505 (2003).
[15] A. Pantano, M. C. Boyce, and D. M. Parks, ASME J. Eng. Mater. Technol. **126**, 279 (2004).
[16] S. Ogata and Y. Shibutani, Phys. Rev. B **68**, 165409 (2003).
[17] H. W. Ch. Postma, T. Teepen, Z. Yao, M. Grigoni, and C. Dekker, Science **293**, 76 (2001).
[18] A. Rechefort, Ph. Avouris, F. Lesage, and D. Salabub, Phys. Rev. B **60**, 13824 (1999).
[19] T. W. Tombler, C. W. Zhou, L. Alexseyev, J. Kong, H. Dai, L. Liu, C. S. Jayanthi, M. J. Tang, and S. Y. Wu, Nature (London) **405**, 769 (2002).
[20] H. Dai, J. H. Hafner, A. G. Rinzler, D. T. Colbert, and R. E. Smalley, Nature (London) **384**, 147 (1996).
[21] S. Iijima, C. Brabec, A. Maiti, and J. Bernholc, J. Chem. Phys. **104**, 2089 (1996).
[22] O. Lourie, D. M. Cox, and H. D. Wagner, Phys. Rev. Lett. **81**, 1638 (1998).
[23] C. Bower, R. Rosen, L. Jin, J. Han, and O. Zhou, Appl. Phys. Lett. **74**, 3317 (1999).
[24] B. I. Yakobson, C. Brabec, and J. Bernholc, Phys. Rev. Lett. **76**, 2511 (1996).
[25] D. Srivastava and S. Barnard, *Molecular Dynamics Simulation of Large-Scale Nanotubes on a Shared-Memory Architecture* (ACM Press, New York, 1997).
[26] A. Garg, J. Han, and S. B. Sinnott, Phys. Rev. Lett. **81**, 2260 (1998).
[27] T. Ozaki, Y. Iwasa, and T. Mitani, Phys. Rev. Lett. **84**, 1712 (2000).
[28] Y. Shibutani and S. Ogata, Modell. Simul. Mater. Sci. Eng. **12**, 599 (2004).
[29] T. Xiao, X. Xu, and K. Liao, J. Appl. Phys. **95**, 8145 (2004).
[30] K. M. Liew, C. H. Wong, X. Q. He, M. J. Tan, and M. A. Meguid, Phys. Rev. B **69**, 115429 (2004).
[31] X. Wang, Y. C. Zhang, X. H. Xia, and C. H. Huang, Int. J. Solids Struct. **41**, 6429 (2004).
[32] D. Qian, G. J. Wagner, and W. K. Liu, Comput. Methods Appl. Mech. Eng. **193**, 1603 (2004).
[33] C. Y. Li and T. W. Chou, Mech. Mater. **36**, 1047 (2004).
[34] C. Q. Ru, Phys. Rev. B **62**, 9973 (2000).
[35] T. Chang, G. Li, and X. Guo, Carbon **43**, 287 (2005).
[36] C. Q. Ru, J. Mech. Phys. Solids **49**, 1265 (2001).
[37] C. Q. Ru, J. Appl. Phys. **89**, 3426 (2001).
[38] C. Y. Wang, C. Q. Ru, and A. Mioduchowski, Int. J. Solids Struct. **40**, 3893 (2003).
[39] Q. Han and G. X. Lu, Eur. J. Mech. A/Solids **22**, 875 (2003).
[40] H. S. Shen, Int. J. Solids Struct. **41**, 2643 (2004).
[41] H. Qian, K. Y. Xu, and C. Q. Ru, Int. J. Solids Struct. **42**, 5426 (2005).
[42] X. Q. He, S. Kitipornchai, and K. M. Liew, J. Mech. Phys. Solids **53**, 303 (2005).
[43] C. Y. Wang, C. Q. Ru, and A. Mioduchowski, ASME J. Appl. Mech. **71**, 622 (2004).
[44] N. L. Allinger, J. Am. Chem. Soc. **99**, 8127 (1977).
[45] T. Chang and H. Gao, J. Mech. Phys. Solids **51**, 1059 (2003).
[46] A. R. Leach, *Molecular Modeling: Principles and Applications* (Addison-Wesley Longman, London, 1996).
[47] L. A. Girifalco and R. A. Lad, J. Chem. Phys. **25**, 693 (1956).
[48] L. A. Girifalco, J. Phys. Chem. **95**, 5370 (1991).
[49] C. T. White, D. H. Robertson, and J. W. Mintmire, Phys. Rev. B **47**, 5485 (1993).
[50] S. P. Timoshenko and J. M. Gere, *Theory of Elastic Stability* (McGraw-Hill, New York, 1961).